A DEEP LOOK AT THE T-TYPE BROWN DWARF BINARY ϵ INDI Bab WITH Chandra AND ATCA

M. AUDARD¹, A. BROWN², K. R. BRIGGS³, M. GÜDEL³, A. TELLESCHI³, AND J. E. GIZIS⁴

To appear in the Astrophysical Journal Letters

ABSTRACT

We present deep observations of the nearby T-type brown dwarf binary ϵ Indi Bab in radio with the Australia Telescope Compact Array and in X-rays with the *Chandra* X-ray Observatory. Despite long integration times, the binary (composed of T1 and T6 dwarfs) was not detected in either wavelength regime. We reached 3σ upper limits of 1.23×10^{12} and 1.74×10^{12} erg s⁻¹ Hz⁻¹ for the radio luminosity at 4.8 GHz and 8.64 GHz, respectively; in the X-rays, the upper limit in the 0.1-10 keV band was 3.16×10^{23} erg s⁻¹. We discuss the above results in the framework of magnetic activity in ultracool, low-mass dwarfs.

Subject headings: radio continuum: stars—stars: activity—stars: coronae—stars: individual (ϵ Ind Bab)—stars: low-mass, brown dwarfs—X-rays: stars

1. INTRODUCTION

Magnetic activity is a common feature of late-type stars. The general hypothesis assumes that some magnetic dynamo mechanism ($\alpha\omega$ dynamo) occurs at the interface between the radiative core of the star and its outer convective zone. However, objects with masses below $0.3~M_{\odot}$ (spectral type later than M3) are generally believed to be fully convective, and thus cannot support the $\alpha\omega$ dynamo. Nevertheless, magnetic activity is commonly seen, even in very late M-type objects (e.g., Johnson 1981, 1987; Tagliaferri et al. 1990; Drake et al. 1996; Fleming et al. 2000; Rutledge et al. 2000; Fleming et al. 1993, 2003; Stelzer 2004). An alternative dynamo mechanism (α^2 dynamo), involving turbulent magnetic fields, has been proposed to take place in fully convective objects (e.g., Durney et al. 1993).

Studies of the H α emission (a common tracer of chromospheric activity) in late-type stars have shown a steep decrease for spectral types later than M7 despite their fast rotation (Gizis et al. 2000; Mohanty & Basri 2003). The Xray emission also appears to decrease, although the sample of studied stars is limited (e.g., Fleming et al. 1993, 2003). It was thus a surprise when Berger (2002) found no decline in radio activity between spectral types M3 and L3.5, and even suggested a possible increase in radio luminosity with cooler effective temperature. Recent results seem to support such a trend in late-M/early-L dwarfs (Berger et al. 2005; Burgasser & Putnam 2005). Old T-type brown dwarfs are, therefore, attractive objects to observe, in order to understand magnetic activity in ultracool dwarfs. However, observations of T dwarfs are scarce in the radio and were nonexistent in X-rays.

This paper extends the previous investigations into the T dwarf domain. We present the first observation of a T dwarf in X-rays with the *Chandra* X-ray Observatory along with a deep observation in the radio regime with the Australia Telescope Compact Array (ATCA). Our target, ϵ Ind Bab, is the

closest known brown dwarf and is composed of two objects with spectral types T1 and T6 separated by 0."73 (2.65 AU at a distance of 3.626 pc; Scholz et al. 2003; Smith et al. 2003; Volk et al. 2003; McCaughrean et al. 2004). We list the binary's main characteristics in Table 1. Blank (2005) failed to detect ϵ Ind Bab with ATCA, but our radio observation goes deeper.

2. OBSERVATIONS AND DATA REDUCTION

Despite our best effort to coordinate the *Chandra* and ATCA observations of the ϵ Ind Bab binary, the X-ray observations were delayed by a few days due to satellite safety reasons. A log of the observations is given in Table 2.

2.1. *ATCA*

The ATCA was in a long-baseline configuration (6D); we used 4.8 GHz and 8.64 GHz receivers with bandwidths of 128 MHz. Observing scans ranged from 10 min to 20 min on source, depending on the weather conditions, whereas we used 3 min scans for the phase calibrator. About 5 minutes at the start of each observing round were spent on the flux calibrator. The observing conditions on the first day were average with cloud coverage; however, the last three hours of the first day of observation were essentially useless due to strong winds and a thunderstorm. In contrast, the weather conditions were much better during the second day with generally a cloud-free sky.

We combined both observing rounds and reduced the ATCA data using the MIRIAD software (Sault et al. 1995). We detected 9 sources in the 4.8 GHz map; we used boxes of about 20" width centered on these sources and applied a CLEAN algorithm using uniform weighting. About 5.4 mJy were thus removed in 202 iterations (we stopped when a negative value was encountered). Although no sources were visible in the dirty map at 8.64 GHz, we used the boxes around the first five brightest sources detected at longer wavelengths and performed a CLEAN algorithm. About 0.5 mJy were removed after 38 iterations. The rms noise level in the cleaned maps reached 26.4 and 37.3 μ Jy at 4.8 and 8.64 GHz, respectively. The values are close to the theoretical values (25.1 and 35.6 μ Jy). No source was detected at the expected position of the T-type brown dwarf binary (see Tab. 2 and Fig. 1). Since short duration flares could be missed in the 2-day images, we have generated maps down to 1-hour duration but still detected no source (typical rms noise levels of 120 μ Jy

¹ Columbia Astrophysics Laboratory, Mail code 5247, 550 West 120th Street, New York, NY 10027, audard@astro.columbia.edu

² Center for Astrophysics and Space Astronomy, University of Colorado, Boulder, CO 80309-0389, ab@casa.colorado.edu

³ Paul Scherrer Institut, Villigen & Würenlingen, 5232 Villigen PSI, Switzerland, briggs@astro.phys.ethz.ch, guedel@astro.phys.ethz.ch, atellesc@astro.phys.ethz.ch

⁴ Department of Physics and Astronomy, 223 Sharp Lab, University of Delaware, Newark, DE 19716, gizis@udel.edu

and 155 μ Jy at 4.8 and 8.64 GHz, respectively). Our nondetection limits are consistent with those of Blank (2005) but we went deeper since we observed ϵ Ind Bab about twice as long. At the distance of the binary (3.626 pc), the 3σ upper limits correspond to radio luminosities, L_R , of 1.23×10^{12} and 1.74×10^{12} erg s⁻¹ Hz⁻¹ at 4.8 and 8.64 GHz, respectively.

2.2. Chandra

Chandra observed ϵ Ind Bab at two different times. We reduced both data sets with the CIAO 3.1 software in combination with CALDB 2.29. The data were taken in VERY FAINT mode which allowed us to further reduce the background level. We later merged both event files into one single event file (total exposure of 62.5 ksec). No signal was detected at the expected position of ϵ Ind Bab (Tab. 2); this was confirmed with several source detection algorithms. Figure 2 shows an extract of the *Chandra* ACIS-S image (0.2–8 keV). Blank (2005) tentatively associated the *ROSAT* source 1WGA J220-5647 with ϵ Ind Bab. However, thanks the high spatial resolution of *Chandra*, we assign the *ROSAT* source to a nearby bright X-ray source instead (see Fig. 2). No optical or near-infrared counterpart to this source could be found in Digitized Sky Survey and Two Micron All Sky Survey images.

No events were detected within 1"4 (95% of the encircled energy at 0.3 keV) of the expected position of ϵ Ind Bab in the 0.2-8 keV range. Note that, without the energy filtering, 4 events were detected but all had energies above 10 keV casting severe doubt that they were due to the source rather than the background. Furthermore, increasing the extraction radius to 3'' only allows the detection of a single event. To estimate the background contribution, we used a concentric annulus with an inner radius of 3" and an outer radius calculated such that the annulus' area was 100 times larger than the area of the circle around the binary (i.e, $r_{\text{out}} = 14.$ "3). A total of 77 events were detected; consequently, the scaled estimated background contribution is 0.77 events, i.e., a mean background rate of 0.012 ct ks⁻¹. We then followed the approach of Kraft et al. (1991) to determine the upper confidence limit using a Bayesian confidence level of 95% which corresponded to 2.99 counts. To convert this count rate of 0.048 ct ks⁻¹ into an X-ray luminosity, we used one plasma component with solar photospheric abundances (Grevesse & Sauval 1998) using the APEC 1.3.1 code (Smith et al. 2001) in the XSPEC software (Arnaud 1996). We obtained count rates in the 0.2-8 keV band and X-ray fluxes in the 0.1-10 keV band. The latter fluxes were converted into X-ray luminosities, L_X , using the distance of ϵ Ind Bab. For plasma temperatures of 0.4 to 1.0 keV, the conversion factor is constant, i.e., 6.5×10^{24} erg s⁻¹ per ct ks⁻¹. For cooler plasma temperatures, the conversion factor increases by factors of 1.16, 1.46, 1.74, and 3.25 for kT = 0.3, 0.2, 0.15, and 0.1 keV, respectively. Similarly, the factor increases by 1.20, 1.33, 1.53, and 1.82 for kT = 1.5, 2, 3, and 5 keV, respectively. Therefore, assuming kT = 0.4 - 1.0 keV, we obtain $L_{\rm X} \lesssim 3.16 \times 10^{23}$ erg s⁻¹. In the worst case (kT = 0.1 keV), our upper limit increases to 1.0×10^{24} erg s⁻¹.

3. DISCUSSION

Since the ATCA could not separate the binary and *Chandra* would have barely done so, our upper limits (L_R and L_X) can either be attributed to one binary component or the other. Table 3 gives the upper limits of the luminosity ratios to the bolometric luminosity for each component.

Our radio upper limits, $L_{\rm R}/L_{\rm bol} < 10^{-16.8} - 10^{-16.0}~{\rm Hz^{-1}}$, do

not go as deep as for dMe stars, which are typically detected with ratios of the order of 10⁻¹⁸ Hz⁻¹. However, the limit at 8.64 GHz is deeper for ϵ Ind Ba than the upper limit obtained at 8.46 GHz with the VLA by Berger (2002) for a T6 brown dwarf (our limit at 8.64 GHz for ϵ Ind Bb is, however, equivalent). Berger hypothesized that the radio luminosity relative to the bolometric luminosity would increase with later spectral type, and their strong detection of an L dwarf in radio appears to support this (Berger et al. 2005). Similarly, despite the lack of sensitivity of current radio instruments, such a trend is also suggested in a small survey of southern late-M and L dwarfs (Burgasser & Putnam 2005). On the other hand, our upper limits for T dwarfs do not indicate that this trend continues into the T dwarf domain. Deep observations of T dwarfs can, in principle, be very useful since they provide data points at low $T_{\rm eff}$; however, the exposure required to achieve the necessary sensitivity for comparison with dMe dwarfs (i.e., $L_{\rm R}/L_{\rm bol} < 10^{-18}-10^{-19}~{\rm Hz}^{-1}$) must await the advent of the next generation of radio telescopes.

In contrast, the sensitivity of Chandra allows us to obtain a low $L_{\rm X}/L_{\rm bol}$ ratio. We reach an upper limit about 10-100times lower than the $L_{\rm X}/L_{\rm bol}$ ratios observed in active dMe stars (e.g., Fleming et al. 1995, 2003). In fact, our limit is close to the ratio observed in the Sun (as a star) at its activity maximum and to the ratio observed in early-dM stars that do not show H α in emission (Fleming et al. 1995). Although X-ray observations of ultracool dwarfs are rare (e.g., Rutledge et al. 2000; Schmitt & Liefke 2002; Martín & Bouy 2002; Fleming et al. 2003; Briggs & Pye 2004; Stelzer 2004; Berger et al. 2005), the X-ray emission in such dwarfs appears to decline like the H α emission. Most X-ray detections were actually obtained during flares, with only a few objects detected in quiescence. Our non-detection of the T-type ϵ Ind Bab with Chandra reinforces the view that the X-ray emission in ultracool dwarfs declines significantly with later spectral type.

Berger et al. (2005) suggested that magnetic activity is strong in ultracool dwarfs, in fact much stronger than in dMe stars, but that it manifests itself mostly in the radio, as atmospheric conditions in such dwarfs become unfavorable for H α and X-ray emission due to the decoupling of the magnetic field from the neutral photospheric gas (Meyer & Meyer-Hofmeister 1999; Mohanty et al. 2002). Taken alone, the lack of X-rays from ϵ Ind Bab could, in principle, support this view. However, Berger (2002) noted that fast rotators (> 10 km s⁻¹) have high L_R/L_{bol} ratios. But ϵ Ind Bab does not follow this trend: Smith et al. (2003) found that the T1 component is a fast rotator ($v \sin i = 28 \text{ km s}^{-1}$). Note that the stellar radius and period are similar to those of the L3.5 dwarf detected in radio (but not in X-rays or H α) by Berger et al. (2005). Possibly, the suggested trend observed in late-M/early-L dwarfs does not hold in the old, cool T dwarfs $(T_{\rm eff} = 800 - 1300 \text{ K})$. Our observation thus suggests a physical change in magnetic behavior somewhere in the range of T dwarfs. Alternatively, the observed sample of L and T dwarfs is too limited and sensitivity is lacking.

Magnetically active stars often show a relation between the quiescent X-ray and radio luminosities (Güdel & Benz 1993). The Güdel-Benz relation points toward a close connection between non-thermal electrons observed as gyrosynchrotron emission and the thermal plasma radiating in X-rays. The origin of this connection remains unclear; however, there is increasing evidence that the X-ray emission in magnetically active stars is due to the statistical superposition of flares (e.g.,

Audard et al. 2000; Güdel et al. 2003). In addition, the radio and X-ray light curves of flares are often correlated (e.g., Neupert 1968; Güdel et al. 2002). Thus, coronal heating by flares provides an elegant explanation for the time-average $L_{\rm X}-L_{\rm R}$ relation observed in active stars. However, ultracool dwarfs seem not to follow this relation since they show stronger radio emission with respect to the X-ray emission (e.g., Berger et al. 2001; Berger 2002; Burgasser & Putnam 2005). This indicates either that magnetic activity in such dwarfs is different (Berger et al. 2001, 2005), or possibly that the radio emission mechanism differs significantly from gyrosynchrotron. Indeed, the emission of many flares in M dwarfs can be ascribed to a coherent mechanism (e.g., Kundu et al. 1988). In the case of ϵ Ind Bab, we obtained only upper limits for both radio and X-ray regimes; thus it is unclear whether the T brown dwarfs follow the Güdel-Benz relation or not.

4. CONCLUSIONS

We have presented deep observations of ϵ Ind Bab, a T1+T6 brown dwarf binary at 3.626 pc, in X-rays with *Chandra* and in the radio with ATCA. The binary remained undetected, with upper limits of $L_{\rm X}/L_{\rm bol}\lesssim 10^{-5.4}$ and $10^{-4.7}$ and $L_{\rm R}/L_{\rm bol}\lesssim 10^{-16.8}$ and $10^{-16.2}$ Hz⁻¹ (at 4.8 GHz) for ϵ Ind Ba and Bb, respectively. The non-detection in the radio is in contrast with the trend of increasing $L_{\rm R}/L_{\rm bol}$ with later spectral type suggested by Berger (2002) and Berger et al. (2005) in late-M and L dwarfs. Berger et al. (2005) argued that the neutral atmospheres in ultracool dwarfs lead to unfavorable conditions for the X-ray and H α emissions (Meyer & Meyer-Hofmeister

1999; Mohanty et al. 2002), but not for the radio emission of fast rotators. However, the T1 component in ϵ Ind Bab is a rapid rotator with similar period and radius as the L dwarf detected strongly in the radio (but undetected in X-rays and H α) by Berger et al. (2005). Therefore, our ϵ Ind Bab observations indicate that cool T dwarfs may not follow the trend suggested by Berger and colleagues. However, a definitive conclusion is difficult to reach in view of the limited sample of ultracool dwarfs observed in the radio and in X-rays and of the lack of sensitivity of present radio (and X-ray) instruments.

The Australia Telescope Compact Array is part of the Australia Telescope which is funded by the Commonwealth of Australia for operation as a National Facility managed by CSIRO. Support for this work was provided by the National Aeronautics and Space Administration (NASA) through Chandra Award Number G04-5002X to Columbia University and issued by the Chandra X-ray Observatory Center, which is operated by the Smithsonian Astrophysical Observatory for and on behalf of the NASA under contract NAS8-03060, and by National Science Foundation grant AST-0206367 and NASA grant NAG5-13058 to the University of Colorado. The PSI group acknowledges support from the Swiss National Science Foundation (grants 20-58827.99 and 20-66875.01). We thank two referees (M. Giampapa and an anonmyous one) for useful comments and suggestions that improved the content of this paper. M. A. thanks Scott Wolk and Bob Sault for their efforts to coordinate the *Chandra* and ATCA observations.

REFERENCES

Arnaud, K. A. 1996, in ASP Conf. Ser. 101, Astronomical Data Analysis Software and Systems V, ed. G. Jacoby & J. Barnes (San Francisco: ASP),

Audard, M., Güdel, M., Drake, J. J., & Kashyap, V. L. 2000, ApJ, 541, 396 Berger, E. 2002, ApJ, 572, 503

Berger, E., et al. 2001, Nature, 410, 338

Berger, E., et al. 2001, Nature, 410, 330 Berger, E., et al. 2005, ApJ, submitted, astro-ph/0502384

Blank, D. L. 2005, MNRAS, 354, 913

Briggs, K. R., & Pye, J. P. 2004, MNRAS, 353, 673

Burgasser, A. J., & Putnam, M. E. 2005, ApJ, in press, astro-ph/0502365

Drake, J. J., Stern, R. A., Stringfellow, G., Mathioudakis, M., Laming, J. M., & Lambert, D. L. 1996, ApJ, 469, 828

Durney, B.R., De Young, B.S., & Roxburgh, I.W. 1993, Sol. Phys., 145, 207 Fleming, T. A., Giampapa, M. S., & Garza, D. 2003, ApJ, 594, 982

Fleming, T. A., Giampapa, M. S., & Schmitt, J. H. M. M. 2000, ApJ, 533,

Fleming, T. A., Giampapa, M. S., Schmitt, J. H. M. M., & Bookbinder, J. A. 1993, ApJ, 410, 387

Fleming, T. A., Schmitt, J. H. M. M., & Giampapa, M. S. 1995, ApJ, 450,

Gizis, J. E., Monet, D. G., Reid, I. N., Kirkpatrick, J. D., Liebert, J., & Williams, R. J. 2000, AJ, 120, 1085

Grevesse, N., & Sauval, A. J. 1998, Space Science Reviews, 85, 161

Güdel, M., & Benz, A. O. 1993, ApJ, 405, L63

Güdel, M., Audard, M., Kashyap, V. L., Drake, J. J., & Guinan, E. F. 2003, ApJ, 582, 423

Güdel, M., Audard, M., Skinner, S. L., & Horvath, M. I. 2002, ApJ, 580, L73

Johnson, H. M. 1981, ApJ, 243, 234

Johnson, H. M. 1987, ApJ, 316, 458

Kraft, R. P., Burrows, D. N., & Nousek, J. A. 1991, ApJ, 374, 344

Kundu, M. R., White, S. M., Jackson, P. D., & Pallavicini, R. 1988, A&A, 195, 159

Martín, E. L., & Bouy, H. 2002, NewA, 7, 595

McCaughrean, M. J., et al. 2004, A&A, 413, 1029

Meyer, F., & Meyer-Hofmeister, E. 1999, A&A, 341, L23

Mohanty, S., & Basri, G. 2003, ApJ, 583, 451

Mohanty, S., Basri, G., Shu, F., Allard, F., & Chabrier, G. 2002, ApJ, 571, 469

Neupert, W. M. 1968, ApJ, 153, L59

Rutledge, R. E., Basri, G., Martín, E. L., & Bildsten, L. 2000, ApJ, 538, L141Sault, R. J., Teuben, P. J., & Wright, M. C. H. 1995, Astronomical Society of the Pacific Conference Series, 77, 433

Schmitt, J. H. M. M., & Liefke, C. 2002, A&A, 382, L9

Scholz, R.-D., McCaughrean, M. J., Lodieu, N., & Kuhlbrodt, B. 2003, A&A, 398, L29

Smith, R. K., Brickhouse, N. S., Liedahl, D. A., Raymond, J. C. 2001, ApJ, 556, L91

Smith, V. V., et al. 2003, ApJ, 599, L107

Stelzer, B. 2004, ApJ, 615, L153

Tagliaferri, G., Giommi, P., & Doyle, J. G. 1990, A&A, 231, 131

Volk, K., Blum, R., Walker, G., & Puxley, P. 2003, IAU Circ., 8188, 2

TABLE 1 The ϵ Ind Bab binary

	ϵ Ind Ba	ϵ Ind Bb
Spectral type	T1	Т6
$\log(L_{\mathrm{bol}}/L_{\odot})$	-4.71	-5.35
$T_{\rm eff}$ (K)	1276 ± 35	854 ± 20
Mass (M_{Jup})	47 ± 10	28 ± 7
Radius (R_{\odot})	0.091 ± 0.005	0.096 ± 0.005
Distance (pc)	3.626	
Age (Gyr)	0.8 - 2	

REFERENCES. — See McCaughrean et al. (2004)

 $\begin{array}{c} {\sf TABLE~2} \\ {\sf OBSERVATION\,LOG\,FOR~ATCA~and} \end{array}$

Position of ϵ Ind Bab (Equinox: J2000; Epoch: J2004.93)			
Right ascension	22 ^h 04 ^m 12 ^s 96		
Declination	-56°47′10′′5		
ATCA (Program C1269)			
Observation date	2004 Dec 4 0h30-14h30 UT		
	2004 Dec 5 1h00-13h00 UT		
Antenna configuration	6D		
Bandwidth	128 MHz over 32 channels		
Flux calibrator	PKS J1939-6342		
(ATCA calibrator name)	(1934–638)		
Phase calibrator	PMN J2121-6111		
(ATCA calibrator name)	(2117–61)		
8.64 GHz			
Synthesized beam	$1''90 \times 1''65$		
Position angle	−18.°7		
Theoretical RMS flux	$35.56~\mu\mathrm{Jy}$		
4.80 GHz			
Synthesized beam	3.755×3.701		
Position angle	-16°7		
Theoretical RMS flux	$25.09~\mu\mathrm{Jy}$		
Chandra (ObsId 6171 and 4485)			
Observation date	2004 Dec 7 13h59-21h11 UT		
	2004 Dec 9 00h04-11h35 UT		
Instrument	ACIS-S		
Total exposure	62.4 ksec		
PSF (FWHM)	0."5		
95% EE PSF @ 0.3 keV	1."44		

TABLE 3
UPPER LIMITS OF LUMINOSITIES AND OF LUMINOSITY
RATIOS TO THE BOLOMETRIC LUMINOSITY

Upper limit	ϵ Ind Ba	ϵ Ind Bb
$L_{\text{R,4.8 GHz}}$ (erg s ⁻¹ Hz ⁻¹)	1.23 >	× 10 ¹²
$L_{R,8.64 \text{ GHz}} \text{ (erg s}^{-1} \text{ Hz}^{-1})$		< 10 ¹²
$L_{\rm X,0.1-10~keV}~({\rm erg~s^{-1}})\dots$	3.16	× 10 ²³
$\log(L_{\text{R,4.8 GHz}}/L_{\text{bol}}) (\text{Hz}^{-1}) \ldots$	-16.79^{a}	-16.15 ^a
$\log(L_{R,8.64 \text{ GHz}}/L_{\text{bol}}) \text{ (Hz}^{-1}) \dots$	-16.64^{a}	-16.00^{a}
$\log(L_{X,0.1-10 \text{ keV}}/L_{\text{bol}}) \dots$	-5.38^{a}	–4.74 ^a

^a Ratios calculated by attributing the luminosity upper limits to each component.

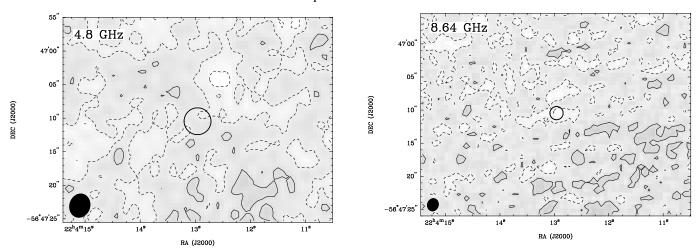


FIG. 1.— Cleaned ATCA maps of the ϵ Ind Bab field at 4.8 GHz (left) and 8.64 GHz (right). Contours are plotted in units of -3, -1, 1, 3, 10 times 26.4 μ Jy and 37.3 μ Jy, respectively. The expected position of the brown dwarf binary (Tab. 2) is shown by open circles of 2'' and 1'' radii, respectively. The beam size is also shown in the bottom left part of each map.

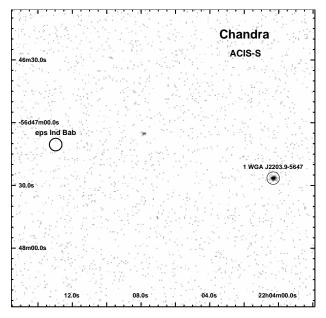


FIG. 2.— Extract of the Chandra ACIS-S image. The expected position of ϵ Ind Bab (Tab. 2) is shown with a circle of 3'' radius.